



RESEARCH ARTICLE

Crystallographic Features and Nature of Luminescence Centres of the Niobate and Tantalate Compounds with Layered Perovskite-Like Structure

Oksana Chukova^{1,*}, Sergiy Nedilko¹, Yuriy Titov¹ and Vadym Sheludko²

¹Taras Shevchenko National University of Kyiv, 64/13, Volodymyrska Str., 01033, Kyiv, Ukraine

²Oleksandr Dovzhenko National Glukhiv University, Sumy Region, 41400, Glukhiv, Ukraine

Received: December 09, 2017

Revised: February 18, 2018

Accepted: February 22, 2018

Abstract:

Aim and Objectives

The ultrafine powders of the perovskite-like layered $A^{II}_3LaM_3O_{12}$ ($A^{II} = Sr, Ba$; $M = Nb, Ta$) compounds have been synthesized by heat treatment of co-precipitated hydroxy-carbonates. The luminescence of these compounds is reported for the first time.

Methods:

Luminescence spectra of all studied compounds are complex and contain two main wide bands with maxima near 2.9 and 2.5 eV. These luminescence bands were assigned to radiation electron transitions in the MoO_6^{7-} molecular groups of different symmetry located in the various lattice positions.

Conclusion:

The energy levels scheme of the MoO_6^{7-} group and related radiation and absorption transitions had been proposed.

Keywords: Tantalate, Niobate, Perovskite, Layer, Luminescence.

1. INTRODUCTION

Multilayer compounds and composites of various nature have always attracted great attention of both scientists and technologists. There are new nanosized layered materials which had been developed for the last decades and they have perspective for both traditional and advanced technologies, *e.g.* industry of consumer goods, high-tech aircraft industry, electronics, biomedicine *etc.* [1 - 4].

The top attention was drawn, *e.g.* to layered carbon materials, and, of course, to graphene among them [5, 6]. Physical properties of such materials are determined not only by structure and interactions between constituents of layers, but these properties also depend on interface structure and interaction between layers. This also applies to the properties of layered inorganic oxide dielectric materials. Therefore, layered perovskite-like oxide compounds have also attracted an interest due to their compositions and unique 2D-like crystallographic parameters that allows to make materials with unusual physical characteristics [6 - 8]. In particular, development of renewable energy sources considers perovskites as promising electrochemistry materials for efficient solar water splitting and nitrogen fixation, *etc.* [5 - 7]. The data about correlation of crystal structure and physical characteristics of such materials could be important for their future developments and applications.

* Address correspondence to this author at the Taras Shevchenko National University of Kyiv, 64/13, Volodymyrska Str., 01033, Kyiv, Ukraine; Tel: 380980611526; E-mail: chukova@univ.kiev.ua

The layered perovskite-like niobates and tantalates are also promising materials for multifunctional usage taking into account a wide range of their interesting properties [9 - 13]. Some applications of the above mentioned compounds could be related to their possible photoluminescence properties, as it is known that some of the niobates and tantalates are able to emit luminescent light [13 - 18]. This luminescence is so-called intrinsic photoluminescence (PL). Intrinsic PL of some materials is one that occurs without incorporation to the material of any additive luminescence agents. The manifestations of the intrinsic PL are known for some oxides containing MO_n molecular groups ($M = W$, Mo, and V) in their crystal lattice [19 - 23]. Unfortunately, according to the intensity of luminescence, niobates and tantalates cannot compete with molybdate, tungsten, or vanadium compounds. However, the niobates and tantalates are characterized by a high absorption cross-section. This feature makes them promising luminescence working media for various purposes, *e.g.* biomedical applications, because such usage requires light transformer materials which characterized by just high efficiency of energy transformation in order to decrease irradiation of living tissues [6, 7]. Search of the ways for increasing luminescence intensity requires a better understanding mechanisms those are responsible for luminescence efficiency of these systems.

Luminescence of some niobate compounds was studied formerly by various authors [14 - 16]. As for the tantalates, their PL was described episodically, *e.g.* concerning $Ba_5Ta_4O_{15}$ [17], $A_2SrTa_2O_7 \cdot nH_2O$ [10], and $YTaO_4$ [13]. The authors found that the PL intensity of those compounds was quite weak. The origin of the tantalate compounds luminescence was usually considered in comparison with luminescence of the same or similar structure niobates compounds *e.g.*, for $Bi/SbMO_4$, Ba/SrM_2O_9 , $Ba_5M_4O_{15}$, Mg/ZnM_2O_6 , $Sr_2M_2O_7$, KMO_3 ($M = Ta$, Nb) compounds [15 - 18, 24 - 26]. Two main PL bands in visible range of the light were ascribed to emission related to radiation electron transitions in NbO_6^{7-} octahedral groups located in different local environment in the crystal lattice [14]. Luminescence mechanisms were supposed to be of the exciton nature, but features of it are still under discussion. The main point of view is the recombination of self-trapped excitons on octahedral groups [18] and emission of the charge transfer vibronic excitons [27]. Strongly distorted corner-sharing octahedral groups are usually characterized by stronger luminescence. The crystal lattice composition essentially influences on luminescence intensity of such compounds. So, some attempts were performed to improve luminescent efficiency by means of cation composition variation [13 - 15, 26]. Aimed to find compositions which could provide higher intensity of luminescence, we studied here layered niobate and tantalate compounds of the same perovskite-like structure. At the same time, different combinations of cations in their cationic and anionic sub-lattices were realized. There were (Sr, Ta), (Sr, Nb), (Ba, Ta), and (Ba, Nb) combinations. So, the set of the $A^{II}_3LaM_3O_{12}$ ($A^{II} = Sr$, Ba; $M = Nb$, Ta) compounds was made and studied. This paper describes results of synthesis, structural characterization and luminescent study of the above noted compounds.

2. EXPERIMENT

The samples under study were synthesized by co-precipitation method. The aqueous solutions of $Sr(NO_3)_2$, $Ba(NO_3)_2$, $La(NO_3)_3$, (high grade) and alcoholic solutions of $NbCl_5$ and $TaCl_5$ were used as initial reagents to made that. There were the next starting ratios of chemical elements (Sr or Ba): La: (Nb or Ta) = 3: 1: 3. The buffer $NH_3 \cdot H_2O + (NH_4)_2CO_3$ aqueous solution of $pH \approx 8.5$ was used as precipitator. The shock heating thermal treatments were carried out for 2 h at 1120 K for $Sr_3LaNb_3O_{12}$ and at 1570 K for all the others compositions [27, 28].

The phase composition and crystal lattice parameters of synthesized compounds were characterized using Shimadzu LabX XRD-6000 ($Cu_K\alpha$ -radiation) diffractometer in $10 < 2\Theta < 90^\circ$ angle range.

Photoluminescence (PL) spectra were measured under excitation of the samples with synchrotron radiation (working range 20 – 3.7 eV) at SUPERLUMI station at HASYLAB (DESY), Hamburg, Germany. Excitation was carried out using 15° Mc Pherson monochromator. Emission was registered using ARC 0.3 m Czerny-Turner monochromator/spectrograph “Spectra Pro 300i” (f/4), liquid nitrogen cooled CCD detector from Princeton Instruments (200-1050 nm) and HAMAMATSU R6358P photomultiplier (200-800 nm) (more experimental details see in [29, 30]). All the emission and excitation spectra were corrected on registration system response.

3. RESULTS

3.1. Structural Peculiarities

The synthesized samples are formed by single crystal phase that we had earlier confirmed using the XRD data [27, 28]. It was found that the $A^{II}_3LaM_3O_{12}$ ($A^{II} = Sr$, Ba; $M = Nb$, Ta) compounds are characterized by layered crystal

structure, that can be described as formed by repetition of some packet of the lattice constituents in direction of axes Z. Each packet (it is named by some authors as “slab”) consists of three perovskite-like layers of the MO_6 octahedrons and A^{II} , La ions. The part of the packet, within the fragment shown in Fig. (1), is called as perovskite-like block [9, 11, 13]. Two of these blocks are completely shown in Fig. (1). (For clarity, we separated them by imaginary planes drawn with dashed lines.) So, we can say that every packet is formed by 3-layered blocks repeated infinitely in XY plane.

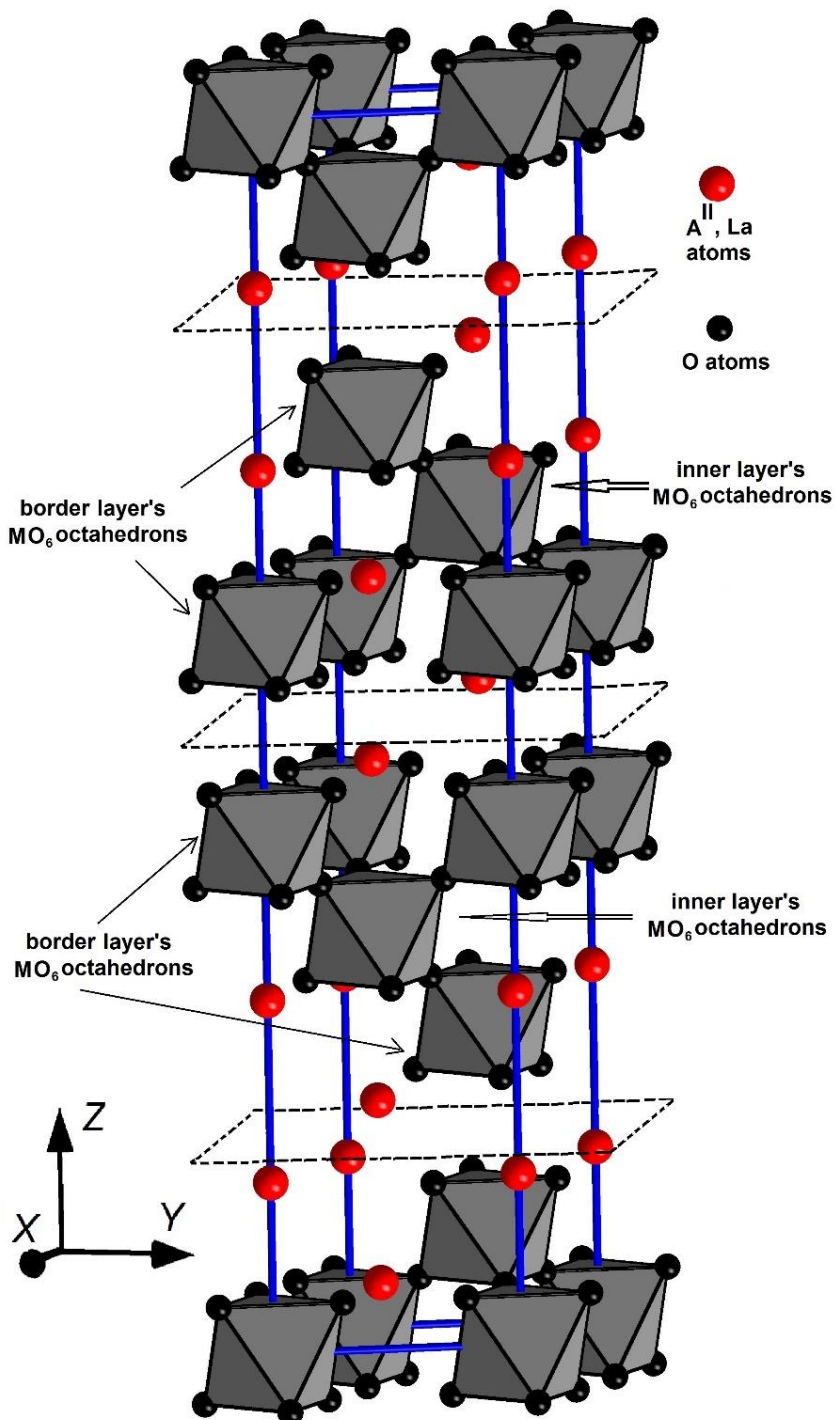


Fig. (1). The fragment of the $\text{A}^{\text{II}}\text{LaM}_3\text{O}_{12}$ ($\text{A}^{\text{II}} = \text{Sr}, \text{Ba}; \text{M} = \text{Nb}, \text{Ta}$) compounds crystal structure.

The MO_6 groups belonging to the same packet are joined by vertices (Fig. 1), while there are no direct connections between the MO_6 octahedrons belonging to neighbour packets. They are linked through - O - (A^{II} , La) - O - interblock bond. This allows us to distinguish the octahedrons of inner layer (inner layer's octahedrons) from the octahedrons of two neighboring layers, which we call as border layer's octahedrons (Fig. 1).

Two of the $\text{A}^{\text{II}}/\text{La}$ cations lie between blocks (one $\text{A}^{\text{II}}/\text{La}$ cation lies above the block and other one lies below the same block). They can be called as non-block cations. The four $\text{A}^{\text{II}}/\text{La}$ cations belong to the block, with one completely, and the other four cations belong also to the adjacent four blocks. Consequently, in the sum we have two cations that lie inside the block. They can be called as internal cations. The described location leads to more significant distortions of the border layer's MO_6 octahedrons compared to the inner layer's ones.

The distortion of the MO_6 groups may effect on luminescence characteristics. Therefore, distortion rates Δ for the $(\text{A}^{\text{II}}, \text{La})\text{O}_{12}$ and of the MO_6 groups were calculated using crystallographic data from the (Table 1) and formulae (1) [31]:

Table 1. Some crystallographic data for the $\text{A}^{\text{II}}_3\text{LaM}_3\text{O}_{12}$ ($\text{A}^{\text{II}} = \text{Sr}, \text{Ba}; \text{M} = \text{Nb}, \text{Ta}$) compounds.

Compound	$\text{Sr}_3\text{LaNb}_3\text{O}_{12}$	$\text{Sr}_3\text{LaTa}_3\text{O}_{12}$	$\text{Ba}_3\text{LaNb}_3\text{O}_{12}$	$\text{Ba}_3\text{LaTa}_3\text{O}_{12}$
Distribution of the $(\text{A}^{\text{II}}, \text{La})$ non-block cations	$0,82\text{Sr} + 0,18\text{La}$	$0,75\text{Sr} + 0,25\text{La}$	$0,75\text{Ba} + 0,25\text{La}$	$0,75\text{Ba} + 0,25\text{La}$
Distribution of the $(\text{A}^{\text{II}}, \text{La})$ internal cations	$0,68\text{Sr} + 0,32\text{La}$	$0,75\text{Sr} + 0,25\text{La}$	$0,75\text{Ba} + 0,25\text{La}$	$0,75\text{Ba} + 0,25\text{La}$
Distortion rates (Δ) of the border layer's MO_6 octahedrons	$72 \cdot 10^{-4}$	$60 \cdot 10^{-4}$	$37 \cdot 10^{-4}$	$18 \cdot 10^{-4}$
Distortion rates (Δ) of the inner layer's MO_6 octahedrons	0	0	0	0
Crystal data source	[27]	[33]	[32]	[11]

$$\Delta = \frac{1}{n} \sum \left[\frac{R_i - \bar{R}}{\bar{R}} \right]^2 \quad (1)$$

where R_i are the cation - Oxygen distances, R is the average distance, n is a coordination number.

The results of calculations are available in the (Table 1). The data on the distribution of the total number of cations A^{II} and La between them (in %) are also given in the (Table 1). According to the data, the $\text{Sr}_3\text{LaNb}_3\text{O}_{12}$ crystal structure is characterized by partially ordered distribution of the Sr and La atoms, when the ions of larger radius (Sr^{2+} ions) are mainly located between the blocks, while the the ions of the smaller radius (La^{3+} ions) are inside the block. On the contrary, the statistical distribution of the alkaline-earth and La ions is characteristic for the $\text{Ba}_3\text{LaM}_3\text{O}_{12}$ ($\text{M} = \text{Nb}, \text{Ta}$) and $\text{Sr}_3\text{LaTa}_3\text{O}_{12}$ compounds [11, 27, 32].

3.2. Luminescence Properties

Emission spectra of both niobate and tantalate samples are presented by wide bands in the 3.5 – 1.7 eV energy range (Fig. 2). Intensity of the tantalate samples emission at room temperature (RT) is quite low. The PL spectra of the $\text{Sr}_3\text{LaTa}_3\text{O}_{12}$ monitored at excitation $E_{\text{ex}} = 6.2$ eV contain three low intensity components with peak position near 2.5, 2.5 and 1.75 eV (Fig. 2, curve3). One more band at 2.85eV appears in the luminescence spectrum measured under excitation $E_{\text{ex}} = 4$ eV. The PL spectra of the $\text{Ba}_3\text{LaTa}_3\text{O}_{12}$ also contain the bands with position of maximum at 2.5, 2.05 and 1.75 eV, but intensity of the niobate samples luminescence is higher at about 5 -10 times if compare with the tantalates emission. The spectra consist of the wide bands at 2.8 and 2.85 eV for the $\text{Sr}_3\text{LaNb}_3\text{O}_{12}$ and $\text{Ba}_3\text{LaNb}_3\text{O}_{12}$ samples, respectively (Fig. 2).

The low temperature ($T = 8$ K) luminescence spectra of the tantalate and niobate samples are similar, but intensity of the niobates luminescence is higher at about 10 times. The main bands of the spectra of the niobates at excitations of $E_{\text{ex}} = 6.2$ eV reach a maximum near 2.75 - 2.7 eV (Fig. 3, curves 3, 4). The long wave length tails of these spectra contain also weak features around 2.1and 1.8 eV. Peak positions of the main PL bands for the tantalates at the noted excitation are at 2.6 – 2.55 and 2.7 – 2.65eV for the $\text{Sr}_3\text{LaTa}_3\text{O}_{12}$ and $\text{Ba}_3\text{LaTa}_3\text{O}_{12}$, respectively (Fig. 3). The PL spectra of the tantalates measured at excitation of $E_{\text{ex}} = 5$ eV show the maxima near 2.5 eV. The low intensity details and shoulder can be also seen at 2.25eV.

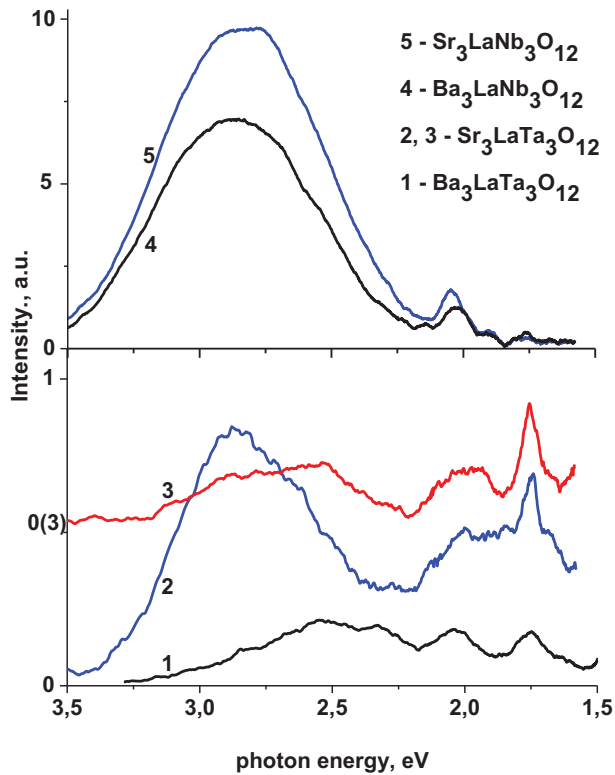


Fig. (2). The PL spectra of the $\text{A}^{\text{II}}_3\text{LaM}_3\text{O}_{12}$ ($\text{A}^{\text{II}} = \text{Sr}, \text{Ba}; \text{M} = \text{Nb}, \text{Ta}$) compounds. $T = 300 \text{ K}$; $E_{\text{ex}} = 4$ (2), 5 (1), and 6.2 eV (3, 4, 5).

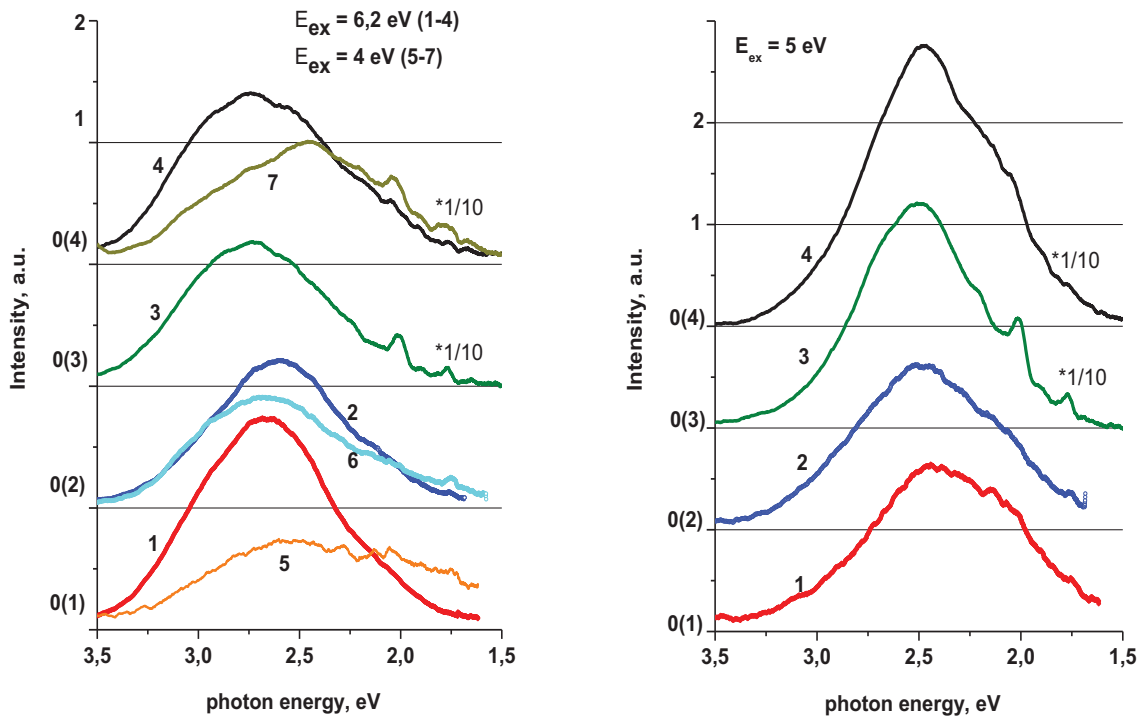


Fig. (3). The PL spectra of the $\text{Ba}_3\text{LaTa}_3\text{O}_{12}$ (1,5), $\text{Sr}_3\text{LaTa}_3\text{O}_{12}$ (2,6), $\text{Ba}_3\text{LaNb}_3\text{O}_{12}$ (3) and $\text{Sr}_3\text{LaNb}_3\text{O}_{12}$ (4,7). $T = 8 \text{ K}$; $E_{\text{ex}} = 6.2$ (1 – 4), 4 eV (5 - 7) for the left part of the Figure; $E_{\text{ex}} = 5 \text{ eV}$ for the right part of the Figure.

The described above the PL peculiarities allowed us to suppose, that all spectra consist of two main bands with maxima positions near 2.9 and 2.5 eV, and variations of these components' contributions determine the position of maximum of the total spectral profile. The relative contribution of the 2.5 eV component is obviously higher for the tantalates than for the niobates (see Fig. 3, left) and when excitation is performed at lower energy of excitation photons. You can pay attention to the curves 5, 7 on the Fig. (3) (left) (E_{ex} = 4 eV) and to the Fig. (3) (right) (E_{ex} = 5 eV). The 2.9 eV component is clearly becomes more pronounced, when the niobates are excited at E_{ex} = 6.2 eV (see Fig. 3, curves 3, 4). Besides, we have to suppose that some others the PL bands of the lower intensity influence the spectral shape, particularly they effect on low energy side of the PL spectra (see, the range 1.5 - 2.25 eV of the curves 1, 2, 5, and 7 on the Fig. 3).

Three spectral ranges can be distinguished in the excitation spectra of luminescence monitored at room temperatures of the samples. (The energy of the radiation photons registered at the measuring of the excitation spectra is indicated below as E_{reg}) There are 11.0 - 7.5, 7.5 - 4.5, and 4.5 - 3.5 eV spectral ranges, where the separated excitation bands are located. We are able to clearly state the difference behavior of the excitation bands with maxima near 5.9 and 4.0 eV. The first of them is of high intensity in the spectra of the niobates, while it vanishes in the spectra of the tantalates (please compare the curves 1, 2 and 3, 4 on the Fig. 4). The band at 4.0 eV is strongly enhanced in the spectra of the Sr-containing compounds, if compare with the spectra of Ba-containing compounds. This last effect is observed for both the niobates and tantalates samples.

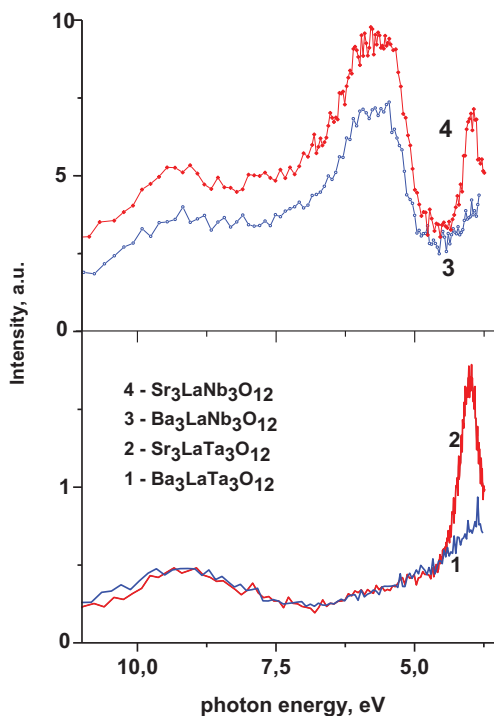


Fig. (4). Excitation spectra of the A''₃LaM₃O₁₂compounds PL(A'' = Sr, Ba; M = Nb, Ta). T = 300 K, E_{reg} = 2.4 (1), 2.9 (2-4) eV.

Excitation spectra registered at low temperature also consist of three main bands located in the spectral ranges near 11–7.0, 7.0–4.8, 4.8–3.7 eV. All the bands are complex and consist of at least two components at 9.0, 8.2; 5.9, 5.2; and 4.5, 4.0 eV, respectively (Fig. 5). The bands in the 11–7.0 eV range undergo minor changes depending on the type of the sample and on the E_{reg} value. For the tantalate compounds the bands at 4.5 and 4.0 eV are of lower intensity in the excitation spectra registered at 2.4 eV compared with the spectra registered at 2.9 eV. Similarly, for the niobate samples the maximum at 5.9 eV has lower intensity in the spectra registered at 2.4 eV compared to the spectra registered at 2.9 eV.

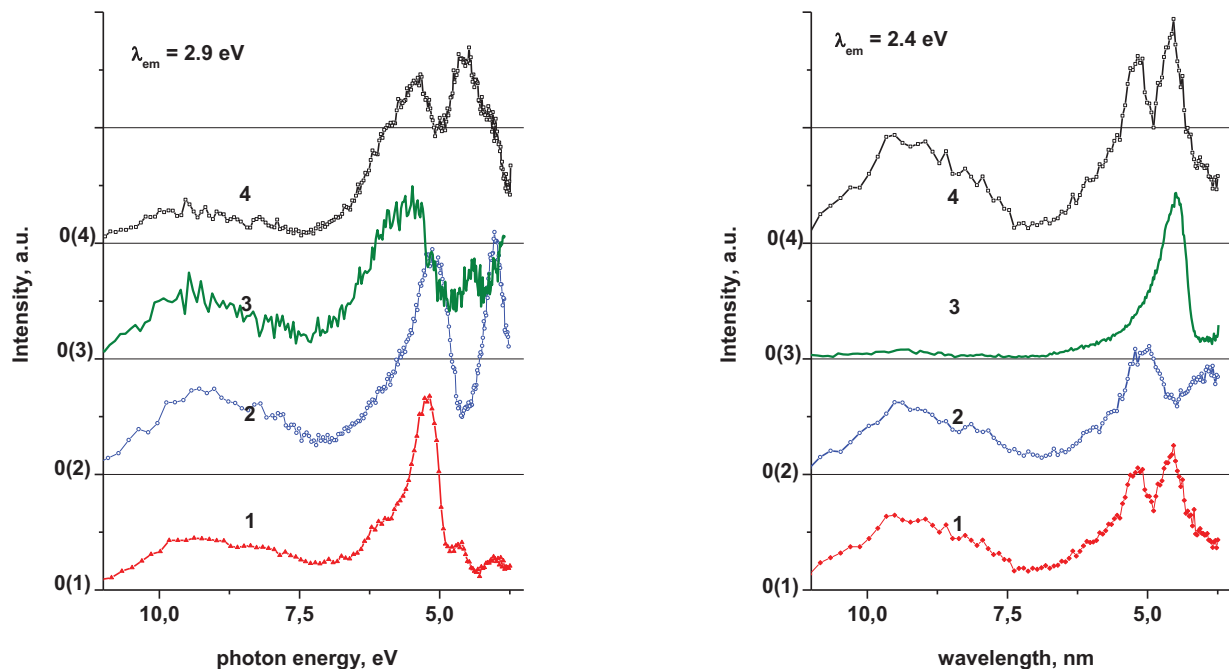


Fig. (5). Excitation spectra of the $\text{Ba}_3\text{LaTa}_3\text{O}_{12}$ (1), $\text{Sr}_3\text{LaTa}_3\text{O}_{12}$ (2), $\text{Ba}_3\text{LaNb}_3\text{O}_{12}$ (3) and $\text{Sr}_3\text{LaNb}_3\text{O}_{12}$ (4); $T = 8 \text{ K}$, $E_{\text{reg}} = 2.9$ (left) and 2.4 eV (right).

3.3. DISCUSSION

The wide band photoluminescence spectra of the investigated tantalate compounds were not reported previously, but above described positions of their emission and excitation bands are similar to those observed previously for the some others layered perovskite-like tantalates [10, 11, 17]. As it was shown formerly, luminescence properties of tantalates and niobates of the same structure are strongly similar and they are usually considered as caused by the same processes [13, 15 - 18]. The excitation and emission transitions in such compounds are known to be mainly related with octahedral niobate and tantalate molecular groups of their crystal lattices. The commonly accepted point of view is that reported two emission bands at 430 and 500 nm (it is equal 2.88 and 2.48 eV, respectively) are connected with electron transitions in MO_6^{7-} groups ($\text{M} = \text{Nb}$ or Ta) located in two different sites of the perovskite – like blocks.

The PL spectra described by us in this work also reveal both noted above the PL bands near 2.9 and 2.5 eV. So, we have to regard these bands as caused by radiation transitions in two different MO_6^{7-} molecular groups of the $\text{A}^{\text{II}}_3\text{LaM}_3\text{O}_{12}$ compounds. In fact, we have already described above that the MO_6^{7-} molecular groups belonging to the inner layer of octahedrons and the molecular groups of the two border layers differ in the level of deformation, symmetry, and composition of the neighborhood environment. Thus, we consider that indicated above differences in the positions of the PL bands and their temperature behavior are caused by different distortion rates of the corresponded MO_6^{7-} groups (Table 1). Really, the MO_6^{7-} groups of the inner layer are close to the O_h octahedral symmetry; whereas stronger distortion of the MO_6^{7-} groups located on the border layers reduces their symmetry to C_{3v} [34]. The reduction of the MO_6^{7-} molecular octahedrons symmetry changes probabilities of the radiation transitions and allows some transitions of lower energy those were forbidden for the octahedrons of the O_h symmetry. In this scheme, we can assign the 2.9 and 2.5 eV emission bands to the $\text{T}_2 \rightarrow \text{A}_1$ and $\text{E} \rightarrow \text{A}_1$ transitions in the MO_6^{7-} groups of the O_h and C_{3v} symmetries, respectively (Fig. 6). Taking into account that relative contribution of the 2.9 eV component is lower for the tantalate compounds, than for the niobate ones, we assume that undistorted tantalate octahedrons, TaO_6^{7-} , are characterized by lower probability of the $\text{T}_2 \rightarrow \text{A}_1$ transitions than undistorted niobate octahedrons, NbO_6^{7-} . We also have observed that the 2.5 eV band is characterized by higher intensity than intensity of the 2.9 eV band at $T = 8\text{K}$ (Fig. 3). This agrees with assumption that strongly distorted octahedral groups are usually characterized by more intensive luminescence [14, 15]. However, the 2.5 eV PL band was not practically observed at room temperature. This can be caused by higher probability of the thermo-activated radiation-less transitions for the more distorted niobate groups [26].

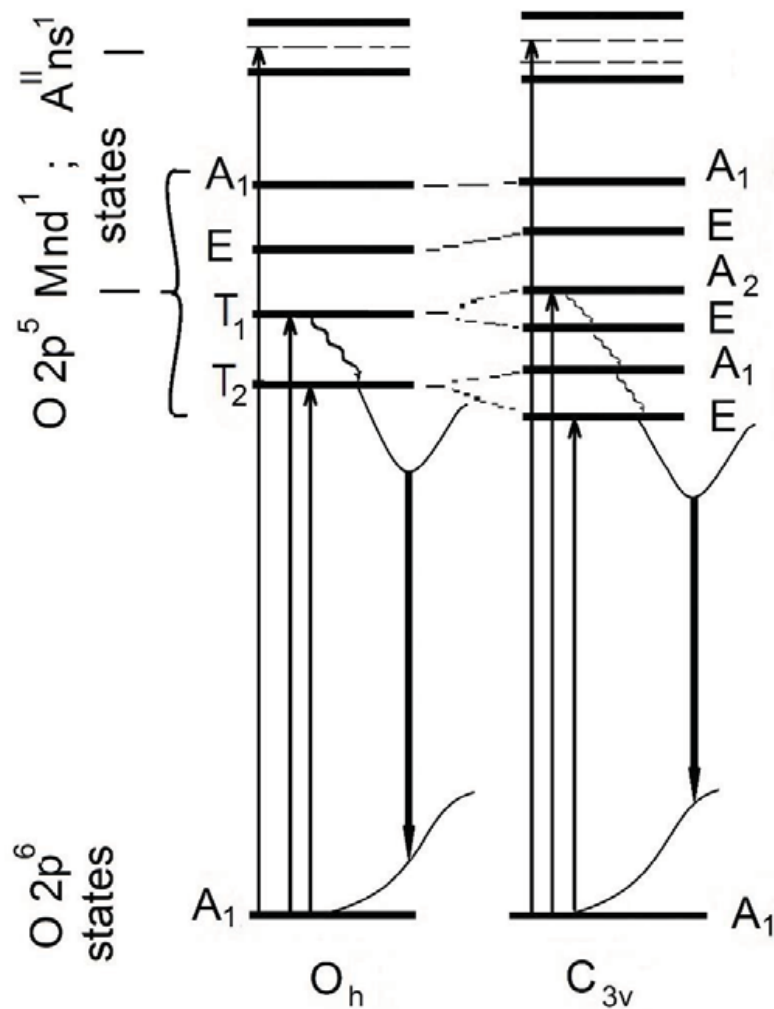


Fig. (6). Scheme of the lowest excited and ground energy levels for the MO_6^{7-} groups and related self-trapped excitons, as well as of the possible electronic absorption and radiation transitions.

The low intensity emission features more clearly observed at room temperature around 2.1 eV and near 1.8 eV are identified as luminescence of the RE^{3+} ions traces. The presence of uncontrolled Eu^{3+} and Pr^{3+} impurities was confirmed by direct laser excitation of the tantalates [35]. We estimate the impurity concentration as lower than $10^{-6}\%$, according to described previously measurements of the luminescence of the solids containing uncontrolled impurities at such low concentrations of the latter [36, 37].

The behavior of the excitation spectra depends heavily on the sample composition, if compared to the PL properties (Figs. 4, 5). It is clearly seen from the excitation spectra measured at 300 K: the excitation band in 6.5 – 4.8 eV energy range is observed only for niobate compounds. The low temperature excitation spectra for the tantalate samples contain the 5.2 eV band, but the 5.9 eV band is observed only for the niobates. So, the properties of the excitation bands in the 6.5–4.8 eV energy range noticeably depend on the M cation type, it is Nb or Ta. We suppose that noted excitation is caused by absorption electron transitions within the MO_6^{7-} groups followed with charge transfer from Oxygen to the central Nb or Ta atoms. There are transitions with electron charge transfer $\text{O}^{2-} \rightarrow \text{M}^{5+}$ from 2p Oxygen orbitals to 5d orbitals of the Ta^{5+} or 4d orbitals of Nb^{5+} ions. The corresponded transitions could be $A_1 \rightarrow E$ and $A_1 \rightarrow T_2$ type, for the 5.9 and 5.2 eV bands, respectively. The above described mechanism of excitation and emission, in fact, determines excitonic nature of observed luminescence. First, the excitation leads to some separation of the charge, then self-localization is realized and, finally, excitation energy releases with luminescence quanta emission. This description is illustrated by the simple scheme of energy levels for the MO_6^{7-} groups and formed self-trapped exciton (Fig. 6).

In fact, we suppose, that luminescence mechanisms in these systems are more complicated. We have pointed out

that earlier when discussed the PL spectra as shown in Fig. (3), and the main PL bands of higher energy and the PL components of lower energy, however, with a weak intensity (1.5 - 2.25 eV) have been discussed. Such situation is typical for intrinsic luminescence of many oxide crystals of chemical composition AXO_n , and the PL was usually explained as superposition of luminescence of regular XO_n ($n = 4, 6$) molecular groups (higher energy bands) and of emission of some defect related luminescence centers (lower energy bands) [19, 38, 39].

The oxygen vacancies are the predominant type of the defects in complex oxides. That is why, we assume that the low energy PL bands can be related to luminescence of the defected MO_6^{7-} group that lost Oxygen - MO_5^{5-} group, or with the MO_6^{7-} octahedron located near the mentioned defective group.

The regular MO_6^{7-} groups can be affected not only by the Oxygen vacancy in neighbor Ta(Nb) – Oxygen octahedron. The vacancies in the cation sublattice, namely A^{II} and La vacancies, can influence electronic states of these groups.

Defect related luminescence, as a rule, is effectively excited in the spectral range below the absorption edge and its excitation is not so effective in the range of band to band electronic transitions. So, according to the data shown on the (Figs. 3 and 4), we can believe that the excitation bands located in the range 3.7 – 4.8 eV are responsible for excitation of luminescence centers related with Oxygen vacancies. Besides, other factors should also be discussed.

We have seen that intensity of the excitation spectra in the 4.7–3.7 eV energy range depends on the A^{II} cation type: that is Sr or Ba. So, the 4.0 eV excitation band is more intensive in the spectra of the Sr-containing samples, while the 4.5 eV band increases in the spectra of the Ba-containing samples. Therefore, the absorption transitions responsible for the long wavelength part of the excitation spectra can be occurred on the MO_6^{7-} groups affected by the A^{II} cation vacancies - V_{AII} . Such possibility can be realized effectively, if luminescence is of exciton nature. Important role of the cations of lattice in luminescence processes in complex center “Cation – Molecular group” was described before for some other oxide crystals, *e.g.* for molybdates and tungstates [19, 40], and also for the other type tantalates [34]. As we pointed above, cation distribution in the $\text{Sr}_3\text{LaNb}_3\text{O}_{12}$ crystal structure differs from the one for the other compounds (Table 1). This feature correlates with behavior of the 4.0 eV excitation band which is intensive only in the spectra of $\text{Sr}_3\text{LaNb}_3\text{O}_{12}$. In such a case, according to data about the cation distribution (Table 1), we can assign the 4.0 eV excitation band to absorption transitions in the centers involving the border MO_6^{7-} -octahedron and vacancy of cation, $\text{MO}_6^{7-}\text{-V}_{\text{AII}}$. Then, the 4.5 eV excitation band may be caused by transitions in the center involving the inner MO_6^{7-} -octahedron and related cation vacancies.

CONCLUSION

The $\text{A}^{\text{II}}_3\text{LaM}_3\text{O}_{12}$ ($\text{A}^{\text{II}} = \text{Sr}, \text{Ba}$, M = Nb, Ta) compounds which are characterized by three-layered perovskite-like structure were studied. There are two types of the MO_6^{7-} octahedrons - constituents of the crystal lattices. Some of them belonging to the inner layer (it lies between two others ones) are of perfect octahedron form. The MO_6^{7-} octahedrons belonging to neighboring (border) layers are distorted. This statement was confirmed by calculation of the distortion rates for corresponding MO_6^{7-} octahedrons. Consequently, two emission bands observed near 2.9 and 2.5 eV were ascribed to the $\text{T}_2 \rightarrow \text{A}_1$ and $\text{E} \rightarrow \text{A}_1$ radiation transitions in the perfect and distorted MO_6^{7-} groups, respectively. The exciton nature of described, so-called intrinsic, luminescence, as well as possible role of the Sr, Ba, and La cations vacancies in luminescence processes of the $\text{A}^{\text{II}}_3\text{LaM}_3\text{O}_{12}$ ($\text{A}^{\text{II}} = \text{Sr}, \text{Ba}$, M = Nb, Ta) compounds were discussed.

The obtained results allowed us to suppose that the studied compounds can be useful as matrix component for the development of the glass-ceramics luminescent transformers of the light aimed to enhance performance of the WLEDs or solar cells. This elaboration requires future study of luminescence origins. The relation between luminescence characteristics, composition, and structure of the materials under consideration should also be studied in more details.

CONFLICT OF INTEREST

The authors declare no conflict of interest, financial or otherwise.

ACKNOWLEDGEMENTS

Publication is based on the research provided by grant of the State budget through the Ministry of the Education and Science of Ukraine (Project 18BF051-01) and by grant of the State Fund for Fundamental Research of Ukraine (Project F64/44-2016).

REFERENCES

- [1] Yu X, Khalil A, Dang PN, Alsberg E, Murphy WL. Multilayered inorganic microparticles for tunable dual growth factor delivery *Adv Funct Mater* 2014; 24: 3082-309.
- [2] Ajayan PM, Schadler L, Braun PV. Nanocomposites science and technology. Weinheim: Wiley-VCH, Verlag GmbH&Co. KgaA 2003. [<http://dx.doi.org/10.1002/3527602127>]
- [3] Camargo PHC, Satyanarayana KG, Wypych F. Nanocomposites: Synthesis, structure, properties and new application opportunities. *Mater Res* 2009; 12: 1. [<http://dx.doi.org/10.1590/S1516-14392009000100002>]
- [4] Shimojima A, Kuroda K. Structural control of multilayered inorganic-organic hybrids derived from mixtures of alkyltriethoxysilane and tetraethoxysilane. *Langmuir* 2002; 18: 1144-9. [<http://dx.doi.org/10.1021/la0110161>]
- [5] Mukawa K, Oyama N, Shinmi T, Sekine Y. Free-surfactant synthesis of graphene-layered carbon composite and its utilization for electrocatalysis. *Bull Chem Soc Jpn* 2016; 89: 892-8. [<http://dx.doi.org/10.1246/bcsj.20160137>]
- [6] Khan AH, Ghosh S, Pradhan B, *et al.* Two-Dimensional (2D) nanomaterials towards electrochemical nanoarchitectonics in energy-related applications. *Bull Chem Soc Jpn* 2017; 90: 627-48. [<http://dx.doi.org/10.1246/bcsj.20170043>]
- [7] Li J, Li H, Zhan G, Zhang L. Solar water splitting and nitrogen fixation with layered bismuth oxyhalides. *Acc Chem Res* 2017; 50(1): 112-21. [<http://dx.doi.org/10.1021/acs.accounts.6b00523>] [PMID: 28009157]
- [8] Li BL, Setyawati MI, Chen L, *et al.* Directing assembly and disassembly of 2D MoS₂nanosheets with DNA for drug delivery. *ACS Appl Mater Interfaces* 2017; 9(18): 15286-96. [<http://dx.doi.org/10.1021/acsami.7b02529>] [PMID: 28452468]
- [9] Lichtenberg F, Herrnberger A, Wiedenmann K, Mannhart K. Synthesis of perovskite-related layered A_nB_nO_{3n+2} = ABO_x type niobates and titanates and study of their structural, electric and magnetic properties. *J Progress in Solid State Chem* 2001; 29: 1-70. [[http://dx.doi.org/10.1016/S0079-6786\(01\)00002-4](http://dx.doi.org/10.1016/S0079-6786(01)00002-4)]
- [10] Shimizu K, Tsujii Y, Hatamachi T, *et al.* Photocatalytic water splitting on hydrated layered perovskite tantalate A₂SrTa₂O₇·nH₂O (A = H, K, and Rb). *Phys Chem Chem Phys* 2004; 6: 1064-9. [<http://dx.doi.org/10.1039/B312620J>]
- [11] Zhang H, Wu Y, Meng S, Fang L. Crystal structure and microwave dielectric properties of a new A₄B₃O₁₂-type cation-deficient perovskite Ba₃LaTa₃O₁₂. *J Alloys Compd* 2008; 460: 460-3. [<http://dx.doi.org/10.1016/j.jallcom.2007.05.099>]
- [12] Tian H, Jia J, Cui X, Yao B, Zhou Z, Chen D. Temperature influence on the voltage-controlled diffractive property of Mn-doped potassium sodium tantalate niobate crystal. *Opt Mater* 2013; 35: 2425-8. [<http://dx.doi.org/10.1016/j.optmat.2013.06.050>]
- [13] Karsu EC, Popovici EJ, Ege A, *et al.* Luminescence study of some yttrium tantalate-based phosphors. *J Lumin* 2011; 131: 1052-7. [<http://dx.doi.org/10.1016/j.jlumin.2011.01.021>]
- [14] Blasse G, Reveau B. The luminescence of potassium silico-niobates. *J Solid State Chem* 1980; 31: 127-30. [[http://dx.doi.org/10.1016/0022-4596\(80\)90014-6](http://dx.doi.org/10.1016/0022-4596(80)90014-6)]
- [15] Wiegel M, Middel W, Blasse G. Influence of ns² ions on the luminescence of niobates and tantalates. *J Mater Chem* 1995; 5: 981-3. [<http://dx.doi.org/10.1039/jm9950500981>]
- [16] Hsiao YJ, Fang TH, Lin SJ, Shieh JM, Ji LW. Preparation and luminescent characteristic of Li₃NbO₄ nanophosphor. *J Lumin* 2010; 130: 1863-5. [<http://dx.doi.org/10.1016/j.jlumin.2010.04.023>]
- [17] Srivastava AM, Ackerman JF, Beers WW. On the Luminescence of Ba₅M₄O₁₅ (M = Ta⁵⁺, Nb⁵⁺). *J Solid State Chem* 1997; 134: 187-91. [<http://dx.doi.org/10.1006/jssc.1997.7574>]
- [18] Blasse G. The influence of crystal structure on the luminescence of tantalates and niobates. *J Solid State Chem* 1988; 72: 72-9. [[http://dx.doi.org/10.1016/0022-4596\(88\)90010-2](http://dx.doi.org/10.1016/0022-4596(88)90010-2)]
- [19] Chukova O, Nedliko S. Study of RE-impurity effects on exciton luminescence of PWO₄ single crystals grown by Czochralski method. *Opt Mater* 2013; 35: 1735-40.

- [<http://dx.doi.org/10.1016/j.optmat.2013.05.019>]
- [20] Hizhnyi YuA, Nedliko SG, Chornii VP, Slobodyanik MS, Zatovsky IV, Terebilenko KV. Electronic structures and origin of intrinsic luminescence in Bi-containing oxide crystals BiPO_4 , $\text{K}_3\text{Bi}_5(\text{PO}_4)_6$, $\text{K}_2\text{Bi}(\text{PO}_4)(\text{MoO}_4)$, $\text{K}_2\text{Bi}(\text{PO}_4)(\text{WO}_4)$ and $\text{K}_3\text{Bi}(\text{MoO}_4)_4$. *J Alloys Compd* 2014; 614: 420-35.
[<http://dx.doi.org/10.1016/j.jallcom.2014.06.111>]
- [21] Chukova OV, Nedliko SG, Slepets AA, Nedliko SA, Voitenko TA. Synthesis and properties of the $\text{La}_{1-x-y}\text{Eu}_x\text{Ca}_y\text{VO}_4$, ($0 \leq x, y \leq 0.2$) compounds. *Nanoscale Res Lett* 2017; 12(1): 340. [REMOVED HYPERLINK FIELD].
[<http://dx.doi.org/10.1186/s11671-017-2116-7>] [PMID: 28486797]
- [22] Nedliko S, Chornii V, Hizhnyi Yu, Trubitsyn M, Volnyanskaya I. Luminescence spectroscopy and electronic structure of the PbMoO_4 and Pb_2MoO_5 single crystals. *Opt Mater* 2014; 36: 1754-9. [REMOVED HYPERLINK FIELD].
[<http://dx.doi.org/10.1016/j.optmat.2014.03.019>]
- [23] Zorenko Y, Gorbenko V, Voloshinovskii A, et al. Luminescence centers in single crystalline films of $\text{Lu}_3\text{Al}_5\text{O}_{12}$ garnet. *Phys Status Solidi 2005*; 2(c): 105-8.
[<http://dx.doi.org/10.1002/pssc.200460122>]
- [24] Black J. Biological performance of tantalum. *Clin Mater* 1994; 16(3): 167-73.
[[http://dx.doi.org/10.1016/0267-6605\(94\)90113-9](http://dx.doi.org/10.1016/0267-6605(94)90113-9)] [PMID: 10172264]
- [25] Marschall R, Soldat J, Busser GW, Wark M. Enhanced photocatalytic hydrogen generation from barium tantalate composites. *Photochem Photobiol Sci* 2013; 12(4): 671-7.
[<http://dx.doi.org/10.1039/C2PP25200G>] [PMID: 23073621]
- [26] Blasse G, Brixner LH. Luminescence of perovskite-like niobates and tantalates. *Mater Res Bull* 1989; 24: 363-6.
[[http://dx.doi.org/10.1016/0025-5408\(89\)90222-5](http://dx.doi.org/10.1016/0025-5408(89)90222-5)]
- [27] Chukova O, Gomenyuk O, Nedliko S, et al. Luminescence processes in $\text{A}_3^{\text{II}}\text{Nb}_3\text{O}_{12}$ ($\text{A}^{\text{II}} = \text{Ba}, \text{Sr}$) layered perovskites. *Opt Mater* 2014; 36: 1709-14.
[<http://dx.doi.org/10.1016/j.optmat.2014.02.001>]
- [28] Titov YuA, Slobodyanik NS, Polubinskii VV, Chumak VV. Mechanisms of the formation of layered $\text{A}_4\text{B}_3\text{O}_{12}$ compounds from co-precipitated hydroxocarbonate and hydroxide systems. *Theor Exp Chem* 2011; 47: 394-8.
[<http://dx.doi.org/10.1007/s11237-012-9233-2>]
- [29] Chukova O, Nedliko SA, Nedliko SG, Sherbatsky V, Voitenko T. Comparable structural and luminescent characterization of the $\text{La}_{1-x}\text{Eu}_x\text{VO}_4$ solid solutions synthesized by solid state and co-precipitation methods. *Diffus Defect Data Solid State Data Pt B Solid State Phenom* 2013; 200: 186-92.
[<http://dx.doi.org/10.4028/www.scientific.net/SSP.200.186>]
- [30] Chukova O, Nedliko S, Scherbatskyi V. Effect of annealing on luminescence properties of the undoped and rare earth doped lead tungstate crystals. *Opt Mater* 2012; 34: 2071-5.
[<http://dx.doi.org/10.1016/j.optmat.2012.04.013>]
- [31] Shannon RD. Revised effective ionic radii and systematic studies of interatomic distances in halides and chalcogenides. *Acta Crystallogr A* 1976; 32: 751-67.
[<http://dx.doi.org/10.1107/S0567739476001551>]
- [32] Rother HJ, Kemmler-Sack S, Treiber U, Cyrus W-R. Über hexagonale perowskite mit kationenfehlstellen. XXI. Die Struktur von $\text{Ba}_4\text{Nb}_2\text{WO}_{12}$ und $\text{Ba}_3\text{LaNb}_3\text{O}_{12}$. *Z Anorg Allg Chem* 1980; 466: 131-8.
[<http://dx.doi.org/10.1002/zaac.19804660115>]
- [33] Antonov VA, Arsenyev PA, Kopilova EK. Crystal structure of $\text{Sr}_3\text{Ta}_3\text{O}_{12}$. *Crystallography* 1990; 35: 630-3.
- [34] Liu GK, Vikhnin VS, Kapphan SE. Anharmonic metastable charge transfer vibronic exciton in potassium tantalate. *J Phys Conf Ser* 2005; 21: 173-6.
[<http://dx.doi.org/10.1088/1742-6596/21/1/028>]
- [35] Chukova O, Nedliko S, Polubinskii V, Scherbatsky V, Titov Y. Synthesis and luminescent investigation of the $\text{Sr}_3\text{Ta}_3\text{O}_{12}$ layered perovskite. *IEEE Xplore Proceedings of Oxide Materials for Electronic Engineering International Conference*. 2012; pp. 209-10.
[<http://dx.doi.org/10.1109/OMEE.2012.6464897>]
- [36] Boyko R, Chukova OV, Gomenyuk OV, Nagornyi PG, Nedliko SG. Origin of red luminescence of some phosphate crystals contained chromium and titanium ions. *Phys Status Solidi* 2005; 2(c): 712-5.
[<http://dx.doi.org/10.1002/pssc.200460272>]
- [37] Mogilevsky R, Nedliko S, Sharafutdinova L, et al. Luminescence study of grown sapphire: from starting material to single crystal. *Phys Status Solidi* 2009; 6(c): s179-83.
[<http://dx.doi.org/10.1002/pssc.200881323>]
- [38] Hizhnyi YuA, Nedliko SG. Investigation of the luminescent properties of pure and defect lead tungstate crystals by electronic structure calculations. *J Lumin* 2003; 102-103: 688-93.
[[http://dx.doi.org/10.1016/S0022-2313\(02\)00625-7](http://dx.doi.org/10.1016/S0022-2313(02)00625-7)]

- [39] Hizhnyi Yu, Oliynik A, Gomenyuk O, *et al.* The electronic structure and optical properties of ABP_2O_7 ($\text{A} = \text{Na}, \text{Li}$) double phosphates. *Opt Mater* 2008; 30: 687-9.
[<http://dx.doi.org/10.1016/j.optmat.2007.02.009>]
- [40] Fujita M, Itoh M, Mitani H, Sangeeta, Tyagi M., Exciton transition and electronic structure of PbMoO_4 crystals studied by polarized light. *Phys Status Solidi* 2010; 247: 405-10. [b].
[<http://dx.doi.org/10.1002/pssb.200945447>]

© 2018 Chukova *et al.*

This is an open access article distributed under the terms of the Creative Commons Attribution 4.0 International Public License (CC-BY 4.0), a copy of which is available at: (<https://creativecommons.org/licenses/by/4.0/legalcode>). This license permits unrestricted use, distribution, and reproduction in any medium, provided the original author and source are credited.